Research Paper

PAIN®

OPEN

Congenital insensitivity to pain: a novel mutation affecting a U12-type intron causes multiple aberrant splicing of *SCN9A*

Margherita Marchi[a,*], Ilaria D'Amato[a], Mirna Andelic[a,b], Daniele Cartelli[a], Erika Salvi[a], Raffaella Lombardi[a], Evren Gumus[c], Giuseppe Lauria[a,d]

Abstract

Mutations in the alpha subunit of voltage-gated sodium channel 1.7 ($Na_V1.7$), encoded by *SCN9A* gene, play an important role in the regulation of nociception and can lead to a wide range of clinical outcomes, ranging from extreme pain syndromes to congenital inability to experience pain. To expand the phenotypic and genotypic spectrum of *SCN9A*-related channelopathies, we describe the proband, a daughter born from consanguineous parents, who had pain insensitivity, diminished temperature sensation, foot burns, and severe loss of nociceptive nerve fibers in the epidermis. Next-generation sequencing of *SCN9A* (NM_002977.3) revealed a novel homozygous substitution (c.377+7T>G) in the donor splice site of intron 3. As the RNA functional testing is challenging, the in silico analysis is the first approach to predict possible alterations. In this case, the computational analysis was unable to identify the splicing consensus and could not provide any prediction for splicing defects. The affected intron indeed belongs to the U12 type, a family of introns characterised by noncanonical consensus at the splice sites, accounting only for 0.35% of all human introns, and is not included in most of the training sets for splicing prediction. A functional study on proband RNA showed different aberrant transcripts, where exon 3 was missing and an intron fragment was included. A quantification study using real-time polymerase chain reaction showed a significant reduction of the $Na_V1.7$ canonical transcript. Collectively, these data widen the spectrum of *SCN9A*-related insensitivity to pain by describing a mutation causing $Na_V1.7$ deficiency, underlying the nociceptor dysfunction, and highlight the importance of molecular investigation of U12 introns' mutations despite the silent prediction.

Keywords: Congenital insensitivity to pain, *SCN9A*, U12-type introns, Loss of function mutation

1. Introduction

Congenital insensitivity to pain (CIP [MIM: 243000]) is an extremely rare autosomal recessive disorder, characterized by the lack of pain-related protective mechanisms against noxious stimuli, which predisposes patients to self-mutilations, burns, and painless fractures. In addition, patients with CIP can also experience anosmia or hyposmia. Congenital insensitivity to pain is caused by biallelic loss-of-function mutations in *SCN9A*, located on chromosome 2 (2q24.3),[23] containing 27 exons and encoding the alpha subunit of the voltage-gated sodium channel 1.7 ($Na_V1.7$). Conversely, mutations inducing a gain of function in $Na_V1.7$ have been shown to cause Mendelian human pain disorders, such as inherited erythromelalgia[6,24] and paroxysmal extreme pain disorder.[10] The channel $Na_V1.7$ is predominantly expressed in the peripheral nervous system and olfactory sensory neurons and shares structural similarity with other mammalian voltage-gated sodium channel subtypes ($Na_V1.1$ to $Na_V1.6$, $Na_V1.8$, and $Na_V1.9$).[4,12] Genetic, structural, and functional studies have demonstrated the contribution of $Na_V1.7$ within the spectrum of human pain disorders.[7] Some gain-of-function variants in $Na_V1.7$ have been associated to more common acquired pain disorders such as small fiber neuropathy[9] and painful diabetic neuropathy.[3]

Thirty-one single nucleotide substitutions and 19 ins/del variations in *SCN9A* have been previously identified in subjects with CIP.[20] Most of them are frame-shift, nonsense, or splicing mutations, and all producing nonfunctional truncated $Na_V1.7$ channels. Missense mutations are extremely rare with only 6 intronic variants having been reported, all located in the consensus sequence of splice sites, within 5bp from exon junction,[2,8,13,14,16,21] and only 2 of them are supported by transcript analyses.

We report the molecular characterization of a novel intronic mutation affecting the donor splice site of intron 3, c.377+7T>G (ClinVar: SCV001738328.1), identified in a pediatric patient

Sponsorships or competing interests that may be relevant to content are disclosed at the end of this article.

M. Marchi and I. D'Amato contributed equally to this work.

[a] Neuroalgology Unit, Fondazione IRCCS Istituto Neurologico "Carlo Besta", Milan, Italy, [b] Department of Neurology, School of Mental Health and Neuroscience, Maastricht University Medical Center, Maastricht, the Netherlands, [c] Department of Medical Genetics, Faculty of Medicine, University of Harran, Sanliurfa, Turkey, [d] Department of Medical Biotechnology and Translational Medicine, University of Milan, Milan, Italy

**Corresponding author. Address: 3rd Neurology Unit—Neuroalgology and Pain Genetics Lab, Fondazione IRCCS Istituto Neurologico "Carlo Besta," Via Celoria 11, 20133 Milan, Italy. E-mail address: margherita.marchi@istituto-besta.it (M. Marchi).*

Supplemental digital content is available for this article. Direct URL citations appear in the printed text and are provided in the HTML and PDF versions of this article on the journal's Web site (www.painjournalonline.com).

PAIN 163 (2022) e882–e887

http://dx.doi.org/10.1097/j.pain.0000000000002535

diagnosed with CIP. The affected intron belongs to the U12 family, characterized by a noncanonical AT-AC sequence at the splice sites, recognized by a functionally relevant U12-dependent spliceosome defined as the minor spliceosome. In most of the cases (98.7%), the exon or intron boundary sequences contain GT and AG motifs at the 5′ and 3′ ends of the intron, respectively, whereas noncanonical AT-AC sequences at the splice sites occur only in 0.09% of the human intron splice sites.

Consequently, atypical splice sites are generally not present in the training sets of bioinformatic splicing prediction tools, with a certain number actively excluding such introns from model training.[18,22] Thus, U12-type introns remain largely unexplored, although such introns are enriched in genes that represent a restricted and conserved set of functional classes and pathways related to DNA replication and repair, transcription, RNA processing, translation, cytoskeletal organization, vesicular transport, and voltage-gated ion channel activity. Both the identities of genes carrying U12-type introns and their positions within the genes are evolutionarily conserved.[22]

The aim of this study was to widen the spectrum of pathogenic mutations in CIP syndrome and to provide further insight on the underestimated impact of variants affecting atypical introns.

2. Material and methods

2.1. Case report

The proband, an 8-year-old girl, was born from consanguineous parents (first-degree cousins). From birth, although urinary incontinence was not observed, the patient had a history of frequent urinary tract infections. From infancy, the parents realized their daughter did not react normally to painful stimuli while playing and interacting with the environment. In addition, the patient's susceptibility to burns, which is the key finding of the disease, is clearly seen. The most valuable finding suggesting the disease is that the patient especially puts her hand on the burning stove and does not withdraw her hand despite the third-degree burn that caused tissue loss. The intelligence quotient was 88. The neurological examination showed isolated impairment of nociceptive and thermal sensation. Hearing and smell were normal, as well as tactile and proprioceptive sensation and deep tendon reflexes. Nerve conduction studies showed normal amplitude of sensory and motor action potentials, and needle electromyography showed motor unit potentials with normal morphology on all limbs. Brain magnetic resonance imaging was normal. Abdominal ultrasound revealed lack of ovarian tissue and a hypoplastic uterus.

Previous genetic screening revealed karyotype rearrangement (47, XXX) that explained the urogenital tract abnormalities and found no mutations in *NTRK1* gene. A homozygous mutation c.377+7T>G was identified in *SCN9A* at the beginning of intron 3. Parents were heterozygous carriers of this mutation. This nucleotide variant was not reported either in the literature or in the public mutations database dbSNP (build 154). In an adjacent position, another point mutation located 3bp upstream (c.377+5C>T; rs200972952) is reported as pathogenic in the ClinVar database in association to CIP, although no functional evidence is provided.[8]

2.2. Skin biopsy

Skin biopsy was taken at the distal site of the leg (10 cm above the lateral malleolus in the territory of the sural nerve) using a disposable 3-mm punch under sterile conditions after intradermal anesthesia with lidocaine. Immediately after sampling, the biopsy was submerged in Zamboni fixative (American MasterTech Scientific) and stored at 4°C. Subsequently, samples were rinsed with 20% sucrose cryoprotectant solution and cryosected in 50-μm-thick sections. Intraepidermal nerve fiber density (IENFD) was evaluated on sections immunostained with polyclonal antiprotein gene product 9.5 (1:500, Ultraclone) by using the free-floating protocol.[5,15] Intraepidermal nerve fiber density was calculated on 3 sections by bright-field microscopy.

2.3. Confocal microscopy

Skin biopsy sections were stained with the following primary antibodies: rabbit anti-human PGP 9.5 (1:400) and mouse anti-human collagen IV (clone CIV 22, 1:20, Dako), secondary goat anti-rabbit IgG Alexa 555, goat anti-mouse Alexa 488, and TO-PRO-3 (1:2000, Thermo Fisher Scientific). The images were taken with oil immersion 63x/1.4 NA objective by using an inverted TCS-SP8 confocal microscope (Leica Microsystems).

2.4. Genetic analysis

Genomic DNA from the proband and her mother was extracted from peripheral blood sampling using the Gentra Puregene Blood Kit (QIAGEN), according to the manufacturer's instructions. The presence of the mutation was verified with Sanger sequencing using a primer pair covering *SCN9A* exon 3 and its flanking splice sites (**Table 1**). Amplicons were purified with Illustra ExoProStar 1-Step (GE Healthcare) and bidirectionally sequenced. Intron 2 was amplified using an upstream oligonucleotide at 500bp from exon 3 and a downstream oligonucleotide at the end of intron 2 (**Table 1**). The amplification products were separated on a 2% agarose gel, and DNA fragments were cropped out from the gel and purified using the Invitrogen PureLink Quick Gel Extraction Kit (Thermo Fisher Scientific) and then sequenced. Mutation nomenclature and nucleotide positions are referred to *SCN9A* transcript NM_002977.3 (human reference release GRCh37). Primers were designed by the Primer3Plus online tool.

2.5. Transcript analysis

Total RNA of the proband and her mother was extracted, according to the manufacturer's instructions, from peripheral

Table 1

Primers used for genomic DNA amplification and Sanger sequencing.

	Amplicon size (bp)	Oligo sequence (5′-3′)	T_a (°C)	Cycles n.
Exon 3	346	TGGAGTCTGATGGCAGTGTT—Fw CCAGAGTCTTTCAAGGTGCAA—Rev	57	30
Intron 2	508	ACTCTGACGTTCCTTCAACTT—Fw CTGCAGGAGGAAAAAGAAAGGA—Rev	56	30

Fw, forward primer; Rev, reverse Primer; T_a, annealing temperature; Cycles n., amplification cycles number.

Table 2

Primers used for cDNA amplification and Sanger sequencing.

	Amplicon size (bp)	Oligo sequence (5′-3′)	T_a (°C)	Cycles n.
Exon 2–4	311	AGTGACTTGGAAGCTGGCAA—Fw TTTTTGGTCCAGTCCGGTGG—Rev	57	35
Selective WT	364	TGCAGACAAAAAGACTTTCATAGT—Fw TTCTGTTAAATACGCAAAAACAATGA—Rev	57	35

Fw, forward primer; Rev, reverse primer; T_a, annealing temperature; Cycles n., amplification cycles number. The underlined letters indicate the splice junctions.

blood collected in PAXgene Tubes, using the PAXgene RNA extraction Kit (all by QIAGEN), and processed with the Invitrogen TURBO DNA-free Kit (Thermo Fisher Scientific). Retrotranscription was obtained by using the Invitrogen SuperScript IV VILO cDNA Synthesis Kit (Thermo Fisher Scientific), and the region of interest was amplified with specific oligonucleotides hybridizing exon 2 and exon 4 (**Table 2**). Amplicons were separated on a 4% low-melting agarose gel, different-sized fragments were cropped out, and purified with the Invitrogen PureLink Quick Gel Extraction Kit (Thermo Fisher Scientific) and then sequenced. Selective polymerase chain reaction (PCR) for WT transcript amplification was performed using specific forward oligonucleotide, targeting the junction between exon 2 and exon 3, and a reverse oligonucleotide matching the junction between exon 5 and 6 (**Table 2**). The amplification product was purified with Illustra ExoProStar 1-Step (GE Healthcare) and bidirectionally sequenced. Primers were designed by the Primer3-Plus online tool. All the fragments were sequenced using the Applied Biosystems BigDye Terminator v1.1 Cycle Sequencing Kit on an Applied Biosystems 3130xl Genetic Analyzer System (Thermo Fisher Scientific).

2.6. RNA isolation and quantitative real-time polymerase chain reaction from skin biopsy samples

Total RNA was isolated from the two 50-μm skin biopsy sections per subject using the truXTRAC FFPE total NA Kit-Column (Covaris), according to the manufacturer's instructions. RNA was eluted in 30 μL of Covaris Elution buffer, and the whole amount was reverse-transcribed by the Invitrogen SuperScript VILO cDNA Synthesis Kit (Thermo Fisher Scientific). For real-time PCR, the Applied Biosystems TaqMan Gene expression assay (Thermo Fisher Scientific) was used following the manufacturer's instructions on cDNA specimens in duplicate, using Applied Biosystems TaqMan Fast Advanced Master Mix (Thermo Fisher Scientific) and mix containing specific probes: *SCN9A* spanning exons 2 to 3 (Hs01076716_m1 Life Technologies) and GAPDH (Hs03929097_g1, Life Technologies). RT-qPCR experiments were performed on the Applied Biosystems ViiA 7 Fast Real-Time PCR System (Thermo Fisher Scientific) using the following cycling protocol: enzyme activation on 92°C for 20 seconds, followed by 40 cycles of denaturation at 95°C for 1 second and annealing at 60°C for 20 seconds. Relative quantification was assessed using the mean values of the PCR duplicates for $2^{-\Delta\Delta Ct}$ calculation.

3. Results

The IENFD at the lower limb was normal in the mother (18.9 IENF/mm, cut-off value 7.1 IENF/mm) and reduced in the proband (5.4 IENF/mm, cut-off value 8.4 IENF/mm) (**Fig. 1**). The cut-off values used to assess the epidermal innervation originate from the worldwide normative study[15] and are sex-dependent and age-dependent, starting from 20-year-old subjects. Because IENFD gradually declines with age, this result suggests severe small-fiber reduction in the young patient.

Sanger sequencing confirmed the homozygous mutation c.377+7T>G (ClinVar: SCV001738328.1) in the young patient, whereas the healthy mother was heterozygous (**Fig. 2**). A biological sample was not available from the healthy father.

The in silico splicing prediction analysis on c.377+7T>G (see Supplementary material, available at http://links.lww.com/PAIN/B534) failed to recognize the splice site in this region and was unable to predict any alterations in splicing.

To prove the consequence of the mutation c.377+7T>G on pre-RNA maturation, we focused on *SCN9A* transcript analysis in the proband, her mother, and 1 unrelated healthy control, which revealed the presence of a band weighted approximately between 300 and 320bp, as expected for the 311bp canonical transcript. A second, shorter, band sized to approximately 190bp was present only in the proband and, more subtly, in her mother, but not in the healthy control (**Fig. 3A**). All the bands were cropped out and purified for direct sequencing.

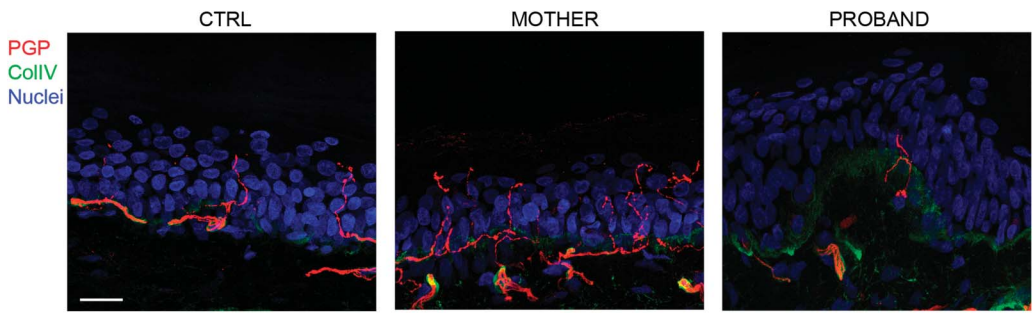

Figure 1. Confocal images of skin biopsies taken from an unrelated healthy control, from the proband's mother, and from the proband, showing severe reduction of intraepidermal nerves innervating the skin of the young proband. Nerve fibers are colored in red (PGP: protein gene product 9.5), basal membrane in green (ColIV: collagen type IV), and cell nuclei in blue (TO-PRO-3). Scale bar: 20 μm.

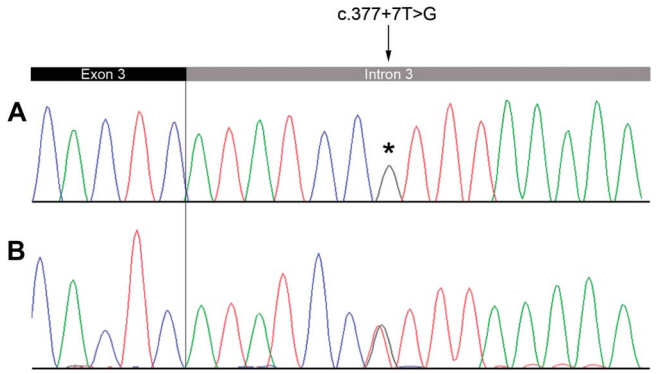

Figure 2. Electropherograms from the genomic sequencing of the exon 3–intron 3 splice junction, showing the presence of the transversion c.377+7T>G, homozygous in the proband (A) and heterozygous in the mother (B). The nucleotide substitution is localized 7 nucleotides downstream from the exon boundary, adjacent to the splicing consensus sequence.

Sanger sequencing of the transcript corresponding to the 300bp band, isolated from the agarose gel (**Fig. 3B**), revealed a misspliced transcript in the proband, characterized by the skipping of exon 3 and a partial retention of intron 2, which is joined to a noncanonical isoform of exon 4 (**Fig. 3C** and Supplementary material, available at http://links.lww.com/PAIN/B534), corresponding to the ENST00000303354.6, from now on it will be named as SK3_INT2_ENST354. The corresponding band in the mother was composed by the same misspliced transcript identified in the proband, together with the 311bp WT transcript (**Figs. 3B and C**). The similar length between the exon skipping (119bp) and the intronic retention (129bp) results in the heterozygous mother as a unique band with a weight comparable with the wild-type allele, ranging from 300 to 320bp. Thus, the sequence of the heterozygous mother showed overlapping electropherograms: one representing the WT transcript and the other corresponding to the misspliced isoform. Sanger sequencing of the lower band showed the presence of a transcript without exon 3 joined with the noncanonical exon 4 splice acceptor site, corresponding to the *SCN9A* isoform ENST00000303354.6. Henceforth it will be conventionally named as SK3_ENST354 (**Fig. 3C**).

The sequencing was extended to intron 2 to exclude that splicing rearrangements were caused by a different nucleotide variant. The sequencing of the intronic region, up to 500bp upstream from exon 3, in the samples, did not reveal any other mutation that could account for partial retention of intron 2.

To investigate whether a minimum amount of the canonical WT transcript was present in the proband, we designed WT-selective primers (**Table 2**) to exclude the amplification of the 2 aberrant transcripts and avoid quantitative bias in PCR amplification. Even if only weakly represented when compared with controls, there was a slight signal of amplification in the proband, which was confirmed

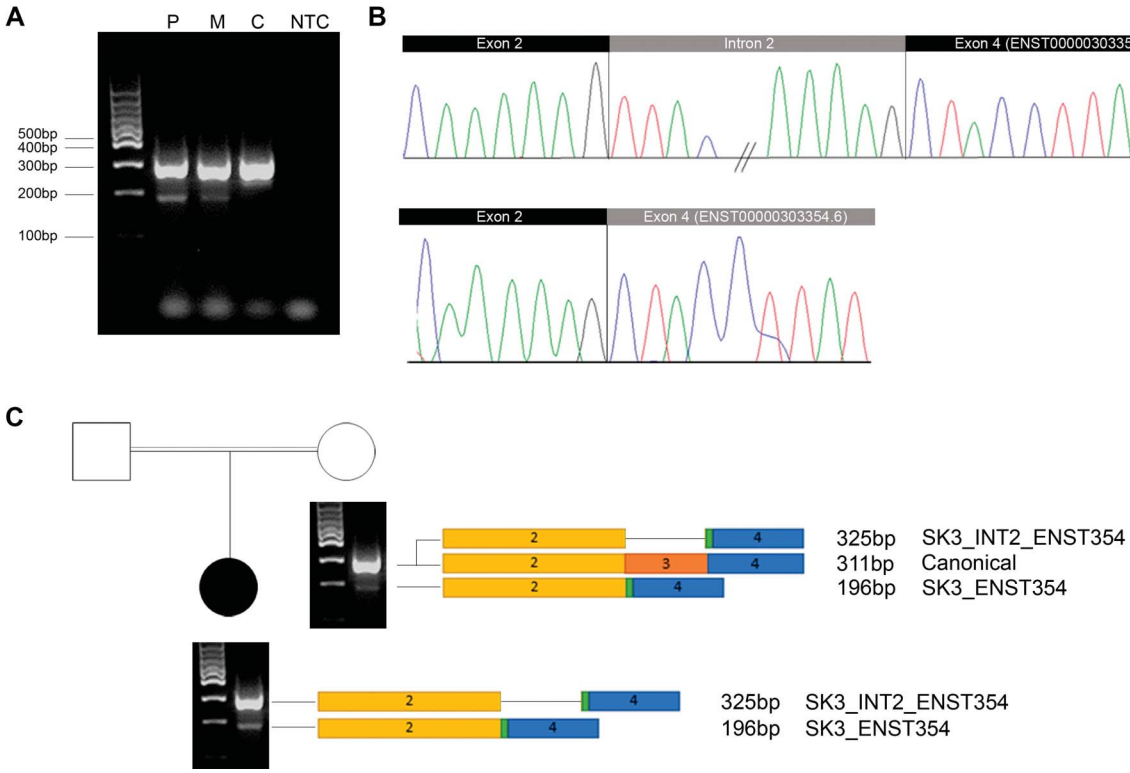

Figure 3. (A) Image of 4% low-melting agarose gel. The upper bands detectable in all the samples have the same dimension of the expected WT transcript. The lower bands, corresponding to a shorter fragment, occurred only in the proband and the mother. Lanes—P: proband; M: mother; C: unrelated control; NTC: no template control. (B) Electropherograms of the 2 misspliced transcripts of *SCN9A* in the proband. Above: Sequence of the SK3_INT2_ENST354 transcript showing the partial retention of intron 2 and the loss of exon 3. Under: Sequence of the SK3_ENST354 transcript characterized by the absence of exon 3. In both the misspliced cases, the noncanonical isoform of exon 4 (ENST00000303354.6) is used. (C) Schematic representation of the transcripts, revealed by sequencing of the bands cropped out from the agarose gel. In the mother, the sequencing of the longer band revealed the presence of 2 overlapped transcripts, one corresponding to the WT allele and the second one with the deletion of exon 3 together with a partial retention of intron 2 and extra 4bp at the beginning of exon 4, corresponding to the noncanonical isoform of SCN9A ENST00000303354.6 (SK3_INT2_ENST354). The shorter band shows a transcript lacking exon 3 and presenting the same noncanonical splice junction isoform ENST00000303354.6 of exon 4 (SK3_ENST354). In the proband, the upper band corresponds to the SK3_INT2_ENST354 transcript and the lower band represents the SK3_ENST354 transcript.

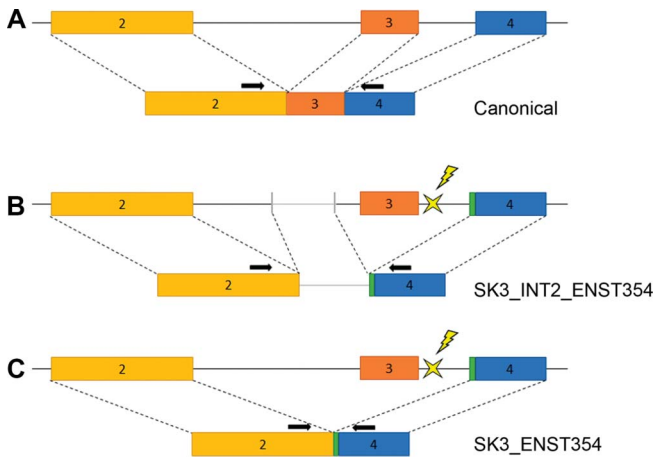

Figure 4. Graphical representation of the alternative transcripts sequenced. (A) Canonical transcript with exon 2, 3, and 4, corresponding to the amplicon 311bp long. (B) SK3_INT2_ENST354 corresponds to the 325bp amplicon and consists of the end of exon 2, a 115bp fragment of intron 2 and an exon 4 with a noncanonical splice site, sited 4bp upstream (ENST00000303354.6). Exon 3 is skipped. (C) SK3_ENST354 represents the shorter amplicon, which is 129bp long, lacks exon 3 and is joined to the same noncanonical exon 4 splice site (ENST00000303354.6).

to correspond to the canonical transcript by Sanger sequencing (**Fig. 4**). To assess the relative amount of WT transcript between the homozygous daughter, the heterozygous mother, and unrelated healthy subjects, relative quantification was performed by TaqMan Assay on RNA extracted from both peripheral blood and skin biopsy. We selected a TaqMan probe capturing selectively the WT transcript, hybridizing the junction between exon 2 and 3. The expression of *SCN9A* in the proband was reduced by 12.5-fold in the skin and by 25-fold in the blood, compared with healthy controls (**Table 3** and Table S1, http://links.lww.com/PAIN/B534).

The translation prediction of the misspliced transcript SK3_INT2_ENST354 showed an out-of-frame reading, starting from lysine 86, which prematurely stops after 2 amino acids (p.Lys86fs2Stop). Similarly, the translation of the transcript SK3_ENST354 ends prematurely with a stop codon after 12 out-of-frame amino acids (p.Lys86fs12Stop), resulting in an overall shortage of functional $Na_V1.7$ (supplementary material, available at http://links.lww.com/PAIN/B534).

4. Discussion

In this study, we described a novel intronic mutation in *SCN9A* leading to complex splicing alterations during transcript maturation as evidenced in the proband.

SCN9A encodes the alpha subunit of the voltage-gated sodium channel $Na_V1.7$, which plays an important role in nociception signalling, and its mutations are associated with a wide range of clinical features, ranging from extreme pain syndromes to congenital inability to experience pain.

Among the 50 mutations in *SCN9A* known to cause CIP, only 6 intronic variants have been reported to date, most without any supporting evidence of pathogenicity. As the functional testing is challenging, many in silico algorithms were developed to test for possible splicing alterations.[1] However, atypical intron types are generally absent in the training sets of the splicing prediction tools, which fail to recognize the canonical splice site in this region and are unable to predict any alterations in splicing. This inability is due to the presence of a noncanonical AT-AC sequence at the splice sites, occurring only in 0.09% of the splice site pairs and characterizing the U12-type introns, processed by the "minor spliceosome", differing from the "major spliceosome" for divergent consensus sequences at 5′ splice sites and branch point.[1] Atypical splice sites globally comprise just 1% of the human introns and therefore do not feature prevalently in training sets for in silico prediction of splicing effects, resulting particularly difficult to predict.[18] Although the relative occurrence of mentioned introns is low, they nonetheless represent a source of pathogenic variants, with mutations affecting the U12 5′ splice sites of introns in the *STK11* and *TRAPPC2* disorder genes being shown to cause Peutz–Jeghers syndrome[11] and spondyloepiphyseal dysplasia tarda,[19] respectively.

This study provides evidence that the *SCN9A* intronic variant c.377+7T>G causes complex aberrant splicing rearrangements, despite the uninformative in silico predictions. Direct sequencing on cDNA showed that the intronic substitution c.377+7T>G induces the generation of several different transcripts, containing cryptic exons and missing the canonical one (**Fig. 4**). As recent research has underlined, when the splice site is weak, as in this case study, a mutation can reveal cryptic splice sites in an adjacent exon or intron which can, in turn, be used in the splicing process. Such splicing mutations are commonly defined as type IV.[1] In this patient, the small amount of WT *SCN9A* transcript is not enough to sustain proper nociceptive sensation, as emerged from the medical history, in which any pain after falling, hitting, and injury was referred. The minimum amount of physiologically functioning sodium channels able to guarantee nociceptive stimuli generation and convey is still unknown, as well as the reduction of sensory fibers in patients with CIP.[17]

In conclusion, our findings widen the spectrum of pathogenic mutations associated with CIP and highlight the importance of underestimated intronic variants, particularly when affecting weak noncanonical splicing consensus. The promising results of the ASO-based therapies demonstrate that the treatment of genetic disorders caused by splicing defects is possible[1] and shed light on the importance of the identification of these mutations in individuals affected by rare and therapeutically challenging diseases.

Table 3

Quantitative real-time PCR analysis of *SCN9A* expression in the skin and in the blood.

Tissue	Sample	Avg Ct SCN9A	Avg Ct GAPDH	ΔCt	ΔΔCt	$2^{-\Delta\Delta Ct}$	Fold change reduction ($-1/2^{-\Delta\Delta Ct}$)
Skin	Proband	39.61	28.03	11.58	3.73	0.08	−12.5
	Mother	38.66	28.15	10.51	2.66	0.16	−6.25
	HCs (group)	36.46	28.61	7.85	0	1	—
Blood	Proband	35.8	23.2	12.7	4.6	0.04	−25
	HCs (group)	32.4	24.3	8.1	0	1	—

The expression of *SCN9A* is normalized vs GAPDH housekeeping gene and is calculated as $2^{-\Delta\Delta Ct}$ using as calibrator the aggregated average expression of a group of 2 healthy controls for the skin and 4 healthy controls for the blood. The relative amount of *SCN9A* is reported as fold change reduction in expression (negative inverse of the $2^{-\Delta\Delta Ct}$). HCs: healthy controls; Avg Ct: average threshold cycle. Ct values for individual samples are reported in supplementary material, Table S1, http://links.lww.com/PAIN/B534.

Furthermore, to the best of our knowledge, there are only 2 reported cases in the literature of human diseases caused by U12-type splice site mutations: the autosomal dominant Peutz–Jeghers syndrome and the X-linked recessive disorder spondyloepiphyseal dysplasia tarda. The variant we have described is the first mutation at the splice sites of U12-type introns associated with an autosomal recessive disorder and within the spectrum of pain-related disorders.

Conflict of interest statement

The authors have no conflicts of interest to declare.

Acknowledgements

The authors acknowledge Ms Maruska Nizzi, British Council, Milan, Italy, for language editing.
This study was supported by grants from the European Union's Horizon 2020 research and innovation programme Marie Sklodowska-Curie grant for PAIN-Net, Molecule-to-man pain network (grant no. 721841). The funders had no role in study design, data collection and analysis, decision to publish, or preparation of the manuscript.
Editorial Policies and Ethical Considerations: Ethical approval was granted from both institutions, and written consent was obtained from the mother also on behalf of the underage patient.
Data Availability Statement: The data that support the findings of this study are available in the supplementary material of this article at http://links.lww.com/PAIN/B534.

Appendix A. Supplemental digital content

Supplemental digital content associated with this article can be found online at http://links.lww.com/PAIN/B534.

Article history:
Received 4 August 2021
Received in revised form 19 October 2021
Accepted 1 November 2021
Available online 15 November 2021

References

[1] Abramowicz A, Gos M. Splicing mutations in human genetic disorders: examples, detection, and confirmation. J Appl Genet 2018;59:253–68.
[2] Bergant G, Maver A, Lovrecic L, Čuturilo G, Hodzic A, Peterlin B. Comprehensive use of extended exome analysis improves diagnostic yield in rare disease: a retrospective survey in 1,059 cases. Genet Med 2018;20:303–12.
[3] Blesneac I, Themistocleous AC, Fratter C, Conrad LJ, Ramirez JD, Cox JJ, Tesfaye S, Shillo PR, Rice ASC, Tucker SJ, Bennett DLH. Rare NaV1.7 variants associated with painful diabetic peripheral neuropathy. PAIN 2018;159:469–80.
[4] Catterall WA. From ionic currents to molecular mechanisms: the structure and function of voltage-gated sodium channels. Neuron 2000;26:13–25.
[5] Devigili G, Rinaldo S, Lombardi R, Cazzato D, Marchi M, Salvi E, Eleopra R, Lauria G. Diagnostic criteria for small fibre neuropathy in clinical practice and research. Brain 2019;142:3728–36.
[6] Dib-Hajj SD, Rush AM, Cummins TR, Hisama FM, Novella S, Tyrrell L, Marshall L, Waxman SG. Gain-of-function mutation in Nav1.7 in familial erythromelalgia induces bursting of sensory neurons. Brain 2005;128:1847–54.
[7] Dib-Hajj SD, Yang Y, Black JA, Waxman SG. The Na(V)1.7 sodium channel: from molecule to man. Nat Rev Neurosci 2013;14:49–62.
[8] Emery EC, Habib AM, Cox JJ, Nicholas AK, Gribble FM, Woods CG, Reimann F. Novel SCN9A mutations underlying extreme pain phenotypes: unexpected electrophysiological and clinical phenotype correlations. J Neurosci 2015;35:7674–81.
[9] Faber CG, Hoeijmakers JGJ, Ahn HS, Cheng X, Han C, Choi JS, Estacion M, Lauria G, Vanhoutte EK, Gerrits MM, Dib-Hajj S, Drenth JPH, Waxman SG, Merkies ISJ. Gain of function Naν1.7 mutations in idiopathic small fiber neuropathy. Ann Neurol 2012;71:26–39.
[10] Fertleman CR, Baker MD, Parker KA, Moffatt S, Elmslie FV, Abrahamsen B, Ostman J, Klugbauer N, Wood JN, Gardiner RM, Rees M. SCN9A mutations in paroxysmal extreme pain disorder: allelic variants underlie distinct channel defects and phenotypes. Neuron 2006;52:767–74.
[11] Hastings ML, Resta N, Traum D, Stella A, Guanti G, Krainer AR. An LKB1 AT-AC intron mutation causes Peutz-Jeghers syndrome via splicing at noncanonical cryptic splice sites. Nat Struct Mol Biol 2005;12:54–9.
[12] Hinard V, Britan A, Schaeffer M, Zahn-Zabal M, Thomet U, Rougier JS, Bairoch A, Abriel H, Gaudet P. Annotation of functional impact of voltage-gated sodium channel mutations. Hum Mutat 2017;38:485–93.
[13] Hou YCC, Yu HC, Martin R, Cirulli ET, Schenker-Ahmed NM, Hicks M, Cohen IV, Jönsson TJ, Heister R, Napier L, Swisher CL, Dominguez S, Tang H, Li W, Perkins BA, Barea J, Rybak C, Smith E, Duchicela K, Doney M, Brar P, Hernandez N, Kirkness EF, Kahn AM, Craig Venter J, Karow DS, Thomas Caskey C. Precision medicine integrating whole-genome sequencing, comprehensive metabolomics, and advanced imaging. Proc Natl Acad Sci U S A 2020;117:3053–62.
[14] Klein CJ, Wu Y, Kilfoyle DH, Sandroni P, Davis MD, Gavrilova RH, Low PA, Dyck PJ. Infrequent SCN9A mutations in congenital insensitivity to pain and erythromelalgia. J Neurol Neurosurg Psychiatry 2013;84:386–91.
[15] Lauria G, Bakkers M, Schmitz C, Lombardi R, Penza P, Devigili G, Smith aG, Hsieh S-T, Mellgren SI, Umapathi T, Ziegler D, Faber CG, Merkies ISJ. Intraepidermal nerve fiber density at the distal leg: a worldwide normative reference study. J Peripher Nerv Syst 2010;15:202–7.
[16] Marchi M, Provitera V, Nolano M, Romano M, Maccora S, D'Amato I, Salvi E, Gerrits M, Santoro L, Lauria G. A novel SCN9A splicing mutation in a compound heterozygous girl with congenital insensitivity to pain, hyposmia and hypogeusia. J Peripher Nerv Syst 2018;23:202–6.
[17] McDermott LA, Weir GA, Themistocleous AC, Segerdahl AR, Blesneac I, Baskozos G, Clark AJ, Millar V, Peck LJ, Ebner D, Tracey I, Serra J, Bennett DL. Defining the functional role of Na V 1.7 in human nociception. Neuron 2019;101:905–19.e8.
[18] Rowlands CF, Baralle D, Ellingford JM. Machine learning approaches for the prioritization of genomic variants impacting pre-mRNA splicing. Cells 2019;8. doi: 10.3390/cells8121513.
[19] Shaw MA, Brunetti-Pierri N, Kádasi L, Kovácová V, Van Maldergem L, De Brasi D, Salerno M, Gécz J. Identification of three novel SEDL mutations, including mutation in the rare, non-canonical splice site of exon 4. Clin Genet 2003;64:235–42.
[20] Stenson PD, Ball EV, Mort M, Phillips AD, Shiel JA, Thomas NST, Abeysinghe S, Krawczak M, Cooper DN. Human gene mutation database (HGMD ®): 2003 update. Hum Mutat 2003;21:577–81.
[21] Sun Y, Man J, Wan Y, Pan G, Du L, Li L, Yang Y, Qiu L, Gao Q, Dan H, Mao L, Cheng Z, Fan C, Yu J, Lin M, Kristiansen K, Shen Y, Wei X. Targeted next-generation sequencing as a comprehensive test for Mendelian diseases: a cohort diagnostic study. Sci Rep 2018;8. doi: 10.1038/s41598-018-30151-z.
[22] Verma B, Akinyi MV, Norppa AJ, Frilander MJ. Minor spliceosome and disease. Semin Cell Dev Biol 2018;79:103–12.
[23] Waxman SG, Merkies ISJ, Gerrits MM, Dib-Hajj SD, Lauria G, Cox JJ, Wood JN, Woods CG, Drenth JPH, Faber CG. Sodium channel genes in pain-related disorders: phenotype-genotype associations and recommendations for clinical use. Lancet Neurol 2014;13:1152–60.
[24] Yang Y, Wang Y, Li S, Xu Z, Li H, Ma L, Fan J, Bu D, Liu B, Fan Z, Wu G, Jin J, Ding B, Zhu X, Shen Y. Mutations in SCN9A, encoding a sodium channel alpha subunit, in patients with primary erythermalgia. J Med Genet 2004;41:171–4.